Current Science
CS 5 (3), 3324-3335 (2025)
Received 13 March 2025 | **Revised 16 April** 2025 | **Accepted 18 May**. 2025 | **Online Available 28 June** 2025
https://doi.org/ 10.52845/CS/2025-5-3-98

Current Science

Current Science

OPEN ACCESS

ISSN(O)2795-8639

Original Article

Research on Optimal Speed Prediction Technology for Submersible Permanent Magnet Synchronous Motor Direct Drive Cavity Pump System

Xinyu Zhao[1,2], Junguo Cui[1,2,*], Fuyuan Li[1,2], Qiankun Huang[1,2], Xiang Gao[1,2], Yu Qu[1,2], Wensheng Xiao[1,2]

[1]**College of Mechanical and Electrical Engineering, China University of Petroleum, Qingdao 266580, China**

[2]**National Engineering Research Center of Marine Geophysical Prospecting and Exploration and Development Equipment, Qingdao 266580, China**

[*]**Corresponding Author: Junguo Cui**

Abstract:
Optimizing the speed control of the submersible permanent magnet synchronous motor (SPMSM) in direct-drive cavity pump systems presents a significant challenge in the digital transformation of oilfield operations. A novel predictive model for determining the optimal pump speed is proposed, integrating an enhanced particle swarm optimization (PSO) algorithm with a neural network. The model zaccurately forecasts the optimal pump speed under diverse operational conditions, thereby improving both the performance and efficiency of the pumping system. Initially, key factors influencing the optimal rotational speed of the cavity pump were analyzed, including crude oil temperature, pressure differential, and volumetric efficiency. Two machine learning approaches—random forest model and the neural network model—were subsequently compared using experimental data to assess their predictive performance. An improved PSO algorithm was introduced, which combines dynamic inertia weight with the Cauchy mutation strategy to address these challenges. The dynamic inertia weight enhances the algorithm's global search capacity during the early stages of optimization, while the Cauchy mutation strategy improves local search efficiency and aids in avoiding local optima. Comparative analysis reveals that the proposed neural network model, integrated with the improved particle swarm optimization algorithm, significantly outperforms the random forest and unoptimized neural network models, demonstrating superior accuracy and stability and enabling more effective control of the SPMSM-driven pump system in oilfield operations.

Keywords: submersible permanent magnet synchronous motor direct drive cavity pump; optimal speed prediction; improved particle swarm optimization algorithm; neural network

1. Introduction

As oil extraction advances to mid and late stages, well conditions become increasingly complex, with more high-inclination, high-sand, and wax-heavy crude oil wells. Current mainstream oil production methods struggle to meet the demands of these complex well conditions. The rod-pumping method faces serious issues, including rod eccentric wear, sucker rod detachment, and tubing abrasion. The structural characteristics of centrifugal pumps make electric submersible centrifugal pump systems prone to jamming and blockage under complex well conditions, with volumetric efficiency sharply decreasing as crude oil viscosity rises.

To address the above issues, cavity pump oil extraction, as an emerging oil extraction method, has gradually emerged in oilfield production operations due to its superior adaptability. Cavity pumps can better cope with high viscosity and high sand content oil wells at low speeds, demonstrating their unique advantages. As the system's power source, submersible motors play a

crucial role in ensuring overall stability. Advances in permanent magnet motor technology have enabled low-speed, high-torque submersible permanent magnet synchronous motors to drive cavity pumps directly, significantly enhancing system efficiency and reliability14, as illustrated in Figure 1.

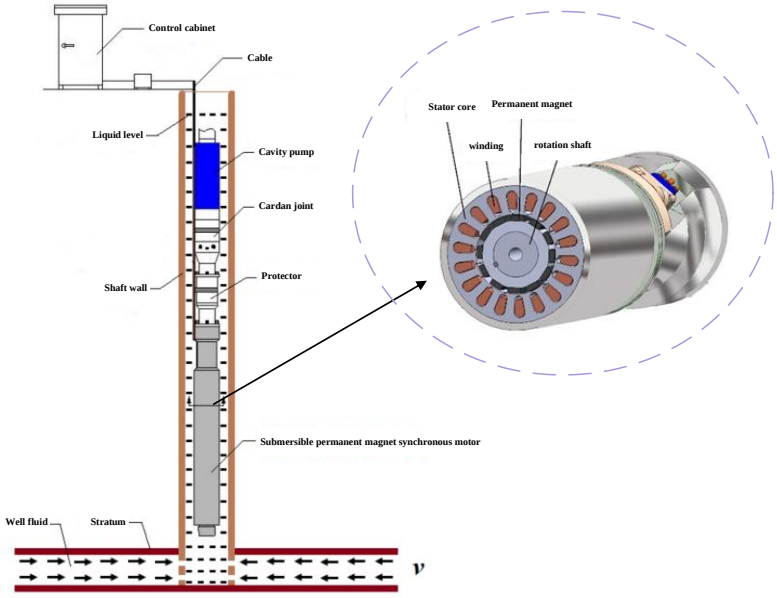

Figure 1. Schematic diagram of submersible permanent magnet synchronous motor direct drive cavity pump system

The research on submersible permanent magnet synchronous motors and direct drive cavity pump systems mainly focuses on Russia58. In 2001, RITEK-ITC LLC, a subsidiary of RITEK JSC, successfully developed the first submersible permanent magnet synchronous motor. However, due to its high speed, a reducer was necessary to lower the speed of the submersible cavity pump, increasing the system's length and failure rate.

In 2006, Borets Company developed both high-speed and low-speed submersible permanent magnet synchronous motors. As of 2023, Borets has installed approximately 22,000 permanent magnet synchronous motors in major oilfields worldwide, achieving significant energy savings estimated at 89,202,040 kW-h annually.

Research on control technology for oil extraction systems began early and has reached a relatively mature stage. With advancements in the Internet of Things (IoT) and artificial intelligence (AI) control technologies, oil extraction systems are gradually evolving towards intelligent control.

Echomer Company in the United States has implemented start-stop control of oil healthy production based on dynamic liquid level changes. Based on dynamic liquid level changes, intermittent pumping operations effectively address "empty pumping" issues in oil production, reducing costs. Grupping et al. suggested that motor speed can be adjusted to real-time dynamic liquid level changes by controlling frequency, thus optimizing drainage intensity and improving oil recovery efficiency9. Baker Company in the U.S. uses sensors to transmit real-time data on dynamic liquid levels and operational data from oil production equipment to a controller. Through analysis, optimal operating conditions for crude oil extraction are determined, enabling digital control of oil production equipment10. A British oil company uses sensors to collect relevant ground and subsurface data, including electrical and dynamic liquid level parameters. After collection, data is transmitted to a ground control center. The control center processes and analyzes this data, generates control instructions, and transmits them to adjust equipment operations, achieving remote control and digitalization of the oil field. Siavashi et al. studied water injection temperature control in heavy oil recovery, examining its impact on recovery rates in addition to traditional water injection rate and bottom hole pressure controls. Their findings showed that optimizing water injection temperature control

significantly improves oil recovery rates11. Purkayastha et al. researched a novel multi-input, multi-output model predictive controller with a steam trap for steam-assisted gravity drainage. Compared to a multi-input, single-output model, this controller improved crude oil recovery by 171%12 .

With the continuous development of computer technology and intelligent monitoring systems, real-time data collected by sensors can be processed with the help of computer intelligent algorithms. Intelligent algorithms use extensive training data to refine their models, ultimately predicting project outcomes13-14. Prediction algorithms are now widely applied across industries, with oil industry research focusing on water injection volume, reserves and production predictions, and equipment failure forecasting. Hu et al. used a BP neural network optimized based on fuzzy clustering and a genetic algorithm to predict crude oil production in oil fields. The stability and prediction accuracy of the optimized neural network were verified through experiments15. Oil healthy production prediction was researched by Li et al., with a comparison made between decision trees, neural decision trees, and artificial neural networks to identify the advantages of each algorithm16 Lu LZ et al. conducted gear fault prediction in oil drilling and production equipment using a self-organizing map (SOM) neural network, proposing an intelligent diagnostic model, establishing life prediction indicators, and verifying the high accuracy of the SOM model for predictive maintenance needs17. Artificial neural networks and support vector machines were compared by Otchere et al. for reservoir characteristic prediction, with support vector machines found to outperform neural networks on limited datasets, and hybrid algorithms being identified as the most effective overall, providing a new approach for reservoir prediction18. The integration of intelligent algorithm prediction with oil and gas extraction is expected to deepen in the future.

In summary, with the development of digitalization and intelligence of oil fields, new requirements are put forward for the control of oil production equipment, especially the direct-drive cavity pump system of submersible permanent magnet synchronous motor. A method is proposed to collect downhole data in real time and use machine learning model to predict the optimal speed of equipment, providing a basis for subsequent speed control.

2 Factors Affecting the Optimal Speed of Submersible Cavity Pump

Given the harsh operating conditions and complex structure and principles of cavity pump equipment, speed adjustment in the cavity pump system must account for various operational influences.

(1) Crude Oil Viscosity

Under consistent conditions, the effect of medium viscosity on cavity pump volumetric efficiency shows a balanced relationship. When viscosity is low, fluid leaks through the cavity pump's internal gaps, reducing output and volumetric efficiency. When the viscosity is moderate, leakage decreases, and the cavity pump fills more effectively, improving volumetric efficiency. When viscosity is too high, lubrication between the rotor and stator rubber is insufficient, increasing wear and shortening the pump's service life.

(2) Crude Oil Temperature

As temperature rises, the stator rubber expands due to thermal expansion, increasing interference between rotor and stator, which enhances sealing, reduces well fluid leakage, and improves the volumetric efficiency of the cavity pump. However, higher temperatures also increase friction between the rotor and stator, accelerating rubber corrosion and wear and shortening the pump's service life.

Additionally, the viscosity of the medium, influenced by temperature, further affects the cavity pump's overall performance.

(3) Pressure Difference and Volumetric Efficiency

When the pressure difference across the cavity pump is low, the sealing chamber functions effectively, resulting in minimal oil leakage and high volumetric efficiency. As the pressure difference rises, especially at a critical threshold, leakage increases due to pressure effects, reducing volumetric efficiency.

During the operation of the cavity pump, due to the influence of pressure difference, the stator liner of the cavity pump defrms. The gap

generated by this deformation can cause leakage of the conveyed liquid, ultimately leading to a decrease in the volumetric efficiency of the cavity pump. The loss part is called the cavity pump volumetric loss. The volumetric efficiency of a cavity pump η_v can be expressed by Eq. (1)

$$\eta_v = \frac{Q_t - q}{Q_t} \quad (1)$$

where, Q_t is the theoretical flow rate of the cavity pump, $m^3 \cdot d^{-1}$; q is the leakage rate of the cavity pump, $m^3 \cdot d^{-1}$.

By incorporating internal structural and operating parameters, Eq. (1) transforms into:

$$1-\eta_v = K_v \frac{\sqrt{p}}{\sqrt{\rho n T}} \sqrt{[1+A\frac{p}{E}(\frac{\delta_0}{D})^{-\beta}]^3[(\frac{\delta_0}{D})^{\beta}]^3}\,\frac{D}{e}\sqrt{\frac{T}{L}} \quad (2)$$

where, K_v is the volume loss coefficient; p is the pump pressure, MPa; ρ is the liquid density, $kg \cdot m^{-3}$; n is the cavity pump speed, $r \cdot min^{-1}$; T is the lead, mm; A and β are constant values; E is the elastic modulus of the liner, $N \cdot mm^{-2}$; δ_0 is the initial interference fit, mm; D is the diameter of the cavity pump rotor, mm; L is the length of the working part of the liner, mm; e is the eccentricity of the pump, mm; T is the temperature constant.

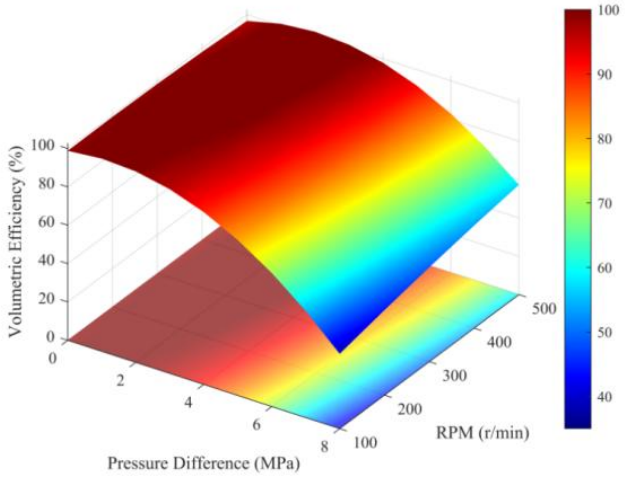

Figure 2 Effect of differential pressure on pump volumetric efficiency at different speeds

Eq. (2) and Figure 2 show that, under similar conditions, higher pump speeds lead to increased volumetric efficiency. Therefore, when the pressure difference across the pump is large, the pump speed can be appropriately increased to maintain efficiency.

(4) Mechanical Efficiency of Cavity Pump

During cavity pump operation, friction between parts causes mechanical losses, directly impacting its mechanical efficiency. The mechanical efficiency η_m of the cavity pump is expressed as follows:

$$\eta_m = \frac{N_t}{N_{ax}} \quad (3)$$

where, N_t is the theoretical power of the cavity pump, kW; N_{ax} is the input power on the shaft of the cavity pump ,kW.

After considering factors such as liquid viscosity, specific heat capacity, and the mechanical loss coefficient, the final result is:

$$\frac{1}{\eta_m} - 1 = K_m \frac{\mu n}{p} \times \frac{1}{(\frac{\delta_0}{D})^{\beta}[1+A\frac{p}{E}(\frac{\delta_0}{D})^{-\beta}]} (\frac{\rho c T_0}{\mu n})^{\frac{2}{3}} \frac{D}{e} \times \frac{L}{T} \quad (4)$$

where, K_m is the mechanical loss coefficient; μ is the liquid dynamic viscosity, Pa·s; c is the liquid mass heat capacity, J/(kg·K).

Eq. (4) shows that, with other parameters constant, an increase in pump speed decreases mechanical efficiency.

Taking into account the above analysis, the pressure difference between the inlet and outlet of the pump, crude oil viscosity, crude oil temperature, and pump volumetric efficiency are selected as the main factors affecting the optimal speed selection of the submersible permanent

magnet synchronous motor direct drive pump system. However, due to the great difficulty of collecting crude oil viscosity and the fact that temperature is an essential factor affecting crude oil viscosity, it is assumed that crude oil viscosity is only related to temperature, and the change in crude oil temperature is approximately used to replace the change in crude oil viscosity. The pressure difference between the inlet and outlet of the pump, the temperature of the crude oil, and the volumetric efficiency of the pump were ultimately selected as the main factors affecting the optimal speed selection of the system.

Due to the complex relationship between these factors and pump rotational speed, establishing a direct relationship is challenging. Thus, machine learning can be applied to train a predictive algorithm model with experimental data to determine the optimal pump speed. The corresponding flowchart is shown in Figure 3.

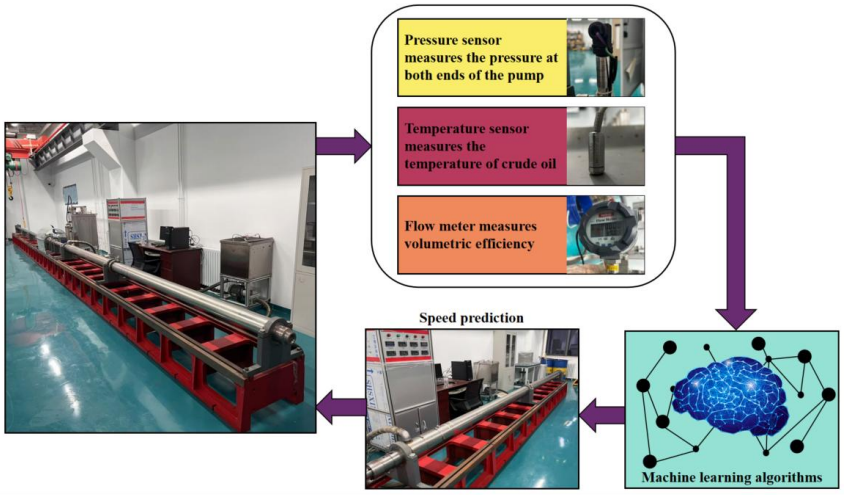

Figure 3. Flow chart for predicting the optimum speed of a progressive cavity pump system

3 Experimental Study on Optimal Speed Prediction

Conduct experimental research to determine the optimal speed prediction of the submersible permanent magnet synchronous motor direct-drive pump system and gather training data for the prediction algorithm model.

As shown in Figure 4, build an experimental platform consisting primarily of a submersible permanent magnet synchronous motor, protector, coupling, pump, solenoid valve group, heating oil tank, system control cabinet, and data acquisition cabinet. The submersible permanent magnet synchronous motor connects to the motor protector and directly drives the pump via the coupling.

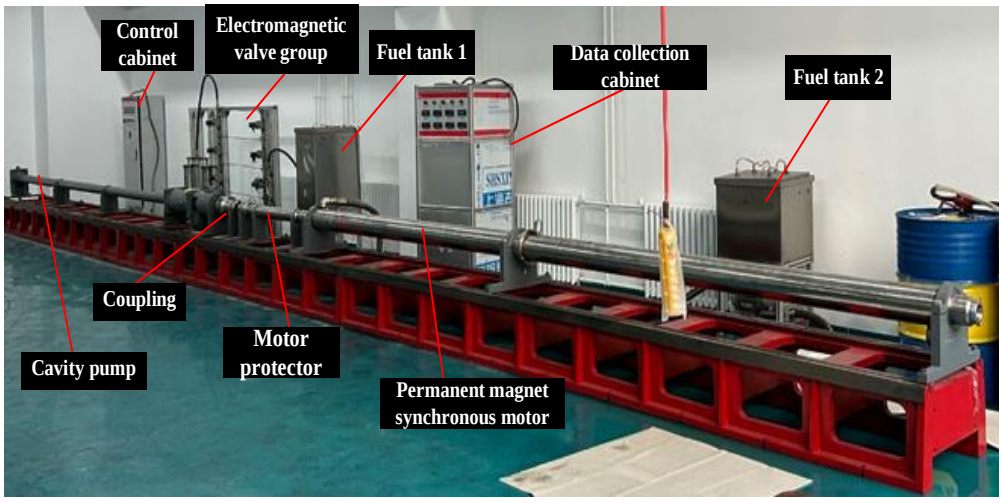

Figure 4 SPMSM direct drive PCP simulation oil recovery system

The experimental platform includes two oil circulation circuits: one for pump circulation connected to oil tank 1 and the other for temperature control of the permanent magnet synchronous motor connected to fuel tank 2. Both tanks are equipped with heating devices, allowing crude oil to be heated via the data acquisition cabinet control, simulating the underground temperature environment. The solenoid valve group adjusts pressure by controlling the opening and closing of valves on both sides, altering the crude oil flow path.

Because the suction port of pump is connected to the heating oil tank, the inlet pressure can be approximated as atmospheric pressure. Install pressure sensors at the pump outlet to measure pressure and temperature sensors in the heated oil tank to measure simulated underground crude oil temperature. A flow meter between the solenoid valve group and oil tank 1 records the pump discharge rate.

Table 1 presents the partial data of the optimal speeds for each influencing factor obtained from the experiment. The first three items serve as inputs for training the prediction algorithm model, while the speed is designated as the output for model training.

Table 1. Selected data from the optimal rotational speed acquisition experiment.

Serial Number	Crude oil temperature/℃	Pump end pressure difference/MPa	volumetric efficiency/%	rotational speed/(r·min^{-1})
1	25.2	5.5	90.5	150
2	25.4	5.8	89.8	153
3	25.5	6.2	88.9	154
4	25.6	6.6	87.5	156
5	25.7	7.2	85.2	158
6	26.1	7.4	84.8	160
7	26.1	7.9	83.2	165
8	26.2	8.2	81.9	165
9	26.4	8.5	80.7	167
10	26.5	8.7	80.1	168

4 Algorithm Predicts Optimal Speed

4.1Comparative analysis of prediction results of random forest algorithm and BP neural network

Due to the experimental data being organized in a specific pattern, it is randomly shuffled and divided into two sets: the training set and the testing set, with a ratio of 80% for training and 20% for testing, to ensure adequate model training and prediction accuracy. To minimize randomness during model training, each of the two models performs five predictions, with the results presented in Figure 5.

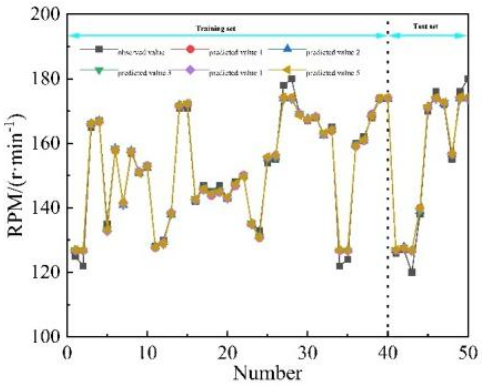

(a)Optimal Rotational Speed Prediction of Random Forest Model

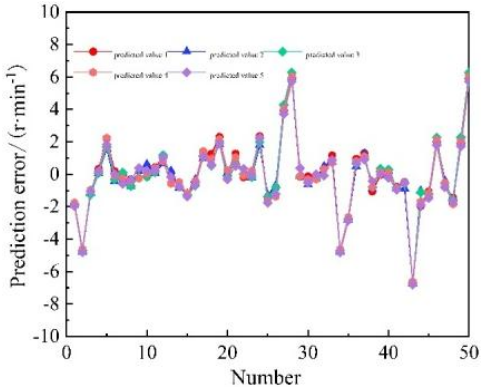

(b)Prediction Error of the Random Forest Model.

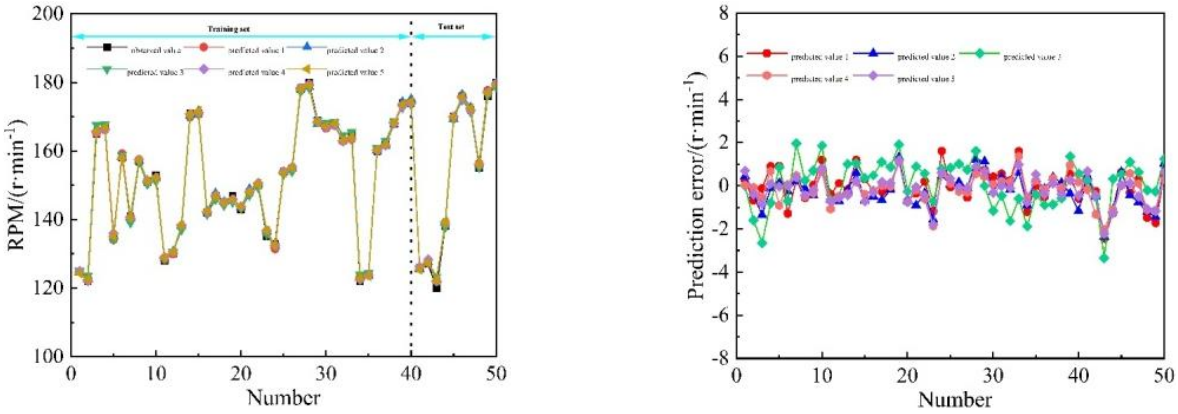

(c)Optimal Rotational Speed Prediction of BP Neural Network Model.

(d)Prediction Error of BP Neural Network Model.

Figure 5. Optimal speed prediction for both prediction models

Figure 5 shows that the neural network prediction algorithm exhibits a smaller prediction error than the random forest regression algorithm; however, its prediction stability is lower, resulting in a more chaotic error curve. In contrast, the random forest algorithm demonstrates better stability, with the error curve showing a tendency to overlap. Thus, while the neural network prediction yields a smaller error, it lacks stability. Conversely, the random forest regression prediction offers better stability but produces a larger prediction error.

Additional testing and evaluation of the random forest and neural network prediction models were performed using the mean squared error (MSE) and the coefficient of determination (R^2). The calculation equations for these metrics are presented in Eqs. (5) and (6), respectively.

$$\mathrm{MSE} = \frac{1}{n}\sum_{t=1}^{n}(\hat{X}_t - X_t)^2 \qquad (5)$$

$$R^2 = 1 - \frac{\sum_{t=1}^{n}(X_t - \hat{X}_t)^2}{\sum_{t=1}^{n}(X_t - \bar{X}_t)^2} \qquad (6)$$

where, $\hat{X}_t$ is the predicted optimal speed of the system; X_t is the optimal speed experimental data; $\bar{X}_t$ is the average value of the optimal speed experimental data.

The two prediction metrics, MSE and R^2, are obtained using the equations above, as presented in Table 2.

Table 2. Test evaluation of the model.

number	random forest algorithm		BP neural network	
	MSE	R^2	MSE	R^2
1	4.63	0.975	0.69	0.987
2	4.65	0.976	0.61	0.988
3	4.78	0.975	1.25	0.986
4	4.68	0.976	0.49	0.988
5	4.56	0.976	0.48	0.988
mean value	4.66	0.9756	0.82	0.9874

4.2 Analysis of Neural Network Prediction Model Results with Improved Particle Swarm Optimization Algorithm

Based on the previous prediction results, it can be concluded that the accuracy of the random forest regression model in predicting the optimal speed of the pump system is lower than that of the neural network model. However, the weight and threshold settings of the neural network significantly affect the accuracy and stability of the predictions, making it challenging to achieve a more accurate final model during training.

Consequently, research is conducted to optimize the weights and thresholds of the neural network. An improved particle swarm optimization algorithm is integrated with the neural network to create an optimization model that uses the neural network's error as the fitness value, aiming to enhance the stability and accuracy of the neural network prediction model.

（1）Introduce a dynamic inertia weight factor

This paper modifies the particle update equation by introducing a dynamic inertia weight factor w, which is crucial at different stages of the algorithm, to enhance the performance of the particle swarm optimization (PSO) algorithm.

In the early stages, a larger inertia factor is assigned to improve global search capability, facilitating the discovery of approximate optimal solutions over a broader range. In the later stages, the inertia weight is reduced to enhance local search capability, ultimately leading to the discovery of the optimal solution. Typically, the initial and final inertia weights are set to 0.9 and 0.4 respectively, at which point the algorithm performance is optimized. The improved algorithm effectively balances global and local search capabilities. The particle update calculation equation is as follows:

$$v_{i+1} = wv_i + c_1 r_1 (pbest_i - x_i) + c_2 r_2 (gbest_i - x_i) \quad (7)$$

Among them, the equation for calculating w is as follows:

$$w = w_s - (w_s - w_e)(\frac{i}{m})^2 \quad (8)$$

where, w_s is the initial inertia weight; w_e is the inertia weight when iterating to the maximum; i is the current iteration count; m is the total number of iterations.

(2) Introducing Cauchy mutation strategy

The standard particle swarm optimization (PSO) algorithm lacks a mutation mechanism, relying instead on mutual cooperation and competition among particles for its optimization process. Consequently, when local extrema and other particles trap a particle and fail to detect it, the algorithm is likely to converge to local optima, preventing the discovery of the global optimum19. Therefore, introducing the Cauchy mutation updates the position of the standard PSO algorithm, enhancing its optimization capability. Cauchy mutation generates a larger mutation step size, increasing the likelihood of escaping from local optima.

The probability density function of the one-dimensional Cauchy distribution is:

$$f_t(x) = \frac{1}{\pi} \frac{t}{t^2 + x^2} \quad (9)$$

Among them, t is a proportional parameter that is greater than 0.

According to the traditional concept of mutation operators, the mutation equation for individuals $X_i = (x_{i1}, x_{i2}, \cdots, x_{in})$ is as follows:

$$x_{ij} = x_{ij} + \eta * C(0,1) \quad (10)$$

Among them, j=1,2,…,n； η is a constant that controls the variation step size; C(0,1)represents the random number generated by the Cauchy distribution function when the proportional parameter t is set to1.

By introducing the Cauchy mutation operator and setting the mutation step size η as the square root of the absolute position value, the position update equation for the Improved Particle Swarm Optimization (IPSO) algorithm is derived as follows:

$$x_{id}^{k+1} = x_{id}^{k} + v_{id}^{k+1} \quad (11)$$

$$x_{id}^{k+1} = x_{id}^{k+1} + \left| x_{id}^{k+1} \right|^{0.5} * C(0,1) \quad (12)$$

The optimization model establishment process is shown in Figure 6.

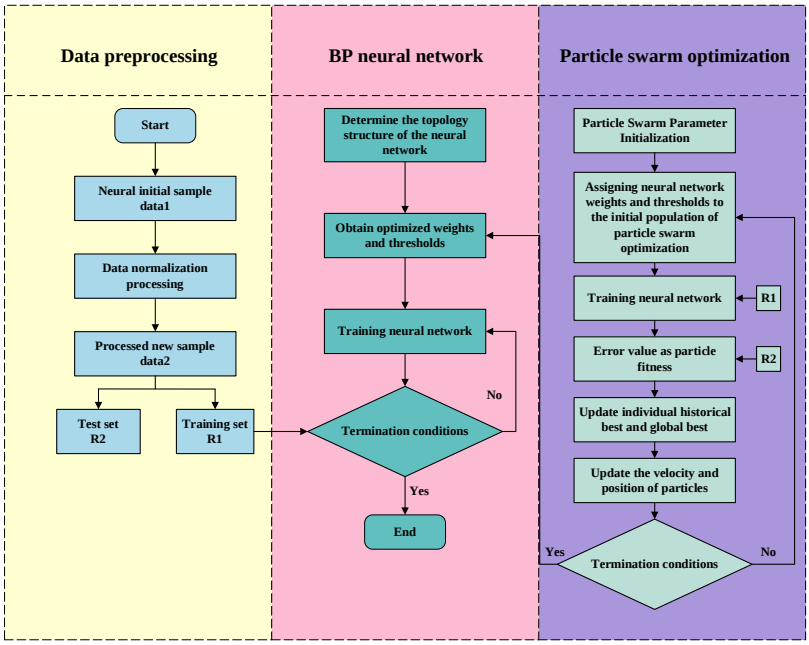

Figure 6. Optimisation flow chart

The steps for establishing the improved neural network prediction algorithm model are as follows:

① Data preprocessing: Normalizing the experimental data effectively prevents a decrease in prediction accuracy due to dimensional differences.

② Set model parameters: Configure relevant parameters for the particle swarm optimization and neural network algorithms, including population size, number of iterations, and neural network structure.

③ Model training: Divide the experimental data into training and testing sets. The training set is used to train the prediction model, enabling it to learn the underlying rules and characteristics of the data, while the testing set evaluates the trained model.

④ Model validation: Evaluate the accuracy of the model predictions based on the results by calculating metrics such as MSE and R2.

The particle swarm algorithm's population size is set to 30，the number of iterations to 500，and the acceleration coefficients c_1 and c_2 to 2. The algorithm begins iterating for optimization, with the iterative process before and after improvement illustrated in Figure 7.

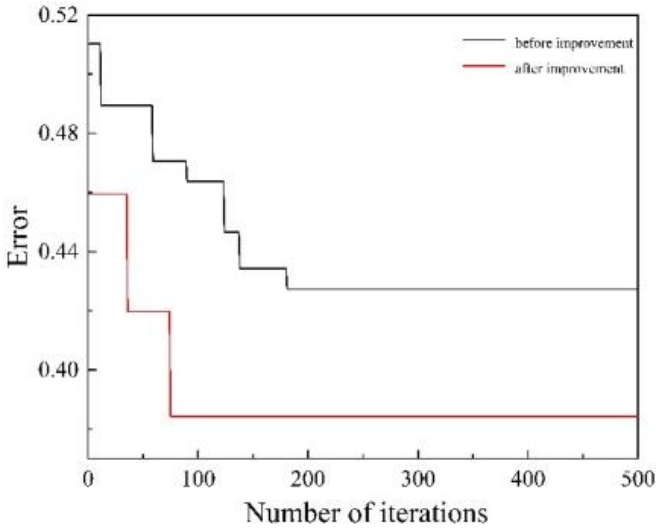

Figure 7 Iterative optimization diagram before and after optimization

Figure 7 indicates that the improved particle swarm algorithm has reduced the number of iterations and enhanced accuracy in the optimization process compared to the previous version.

The weights and thresholds obtained from the iterations are substituted into the neural network prediction model. The optimized neural network model was trained five times, and the prediction results are presented in Figure 8.

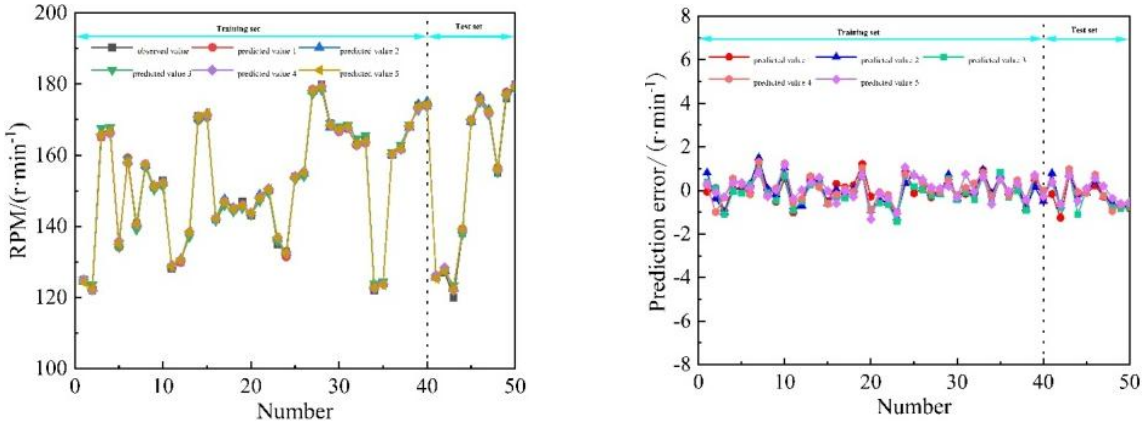

(a)Optimal Rotational Speed Prediction of Optimized Neural Network Prediction Model.

(b)Prediction Error of Optimized Neural Network Prediction Model.

Figure 8. Prediction results of the optimized model

Figure 8 shows that the optimized neural network prediction model exhibits a small prediction error and a high degree of overlap in the error curves, which results in improved prediction stability.

To further demonstrate the superior performance of the optimized prediction model, the mean square error and coefficient of determination for the improved model were calculated using Eqs. (5) and (6). The final comparison results for each prediction model are presented in Table 3.

Table 3. Test evaluation of the model.

number	random forest algorithm		BP neural network		Improving Particle Swarm Optimization Neural Network	
	MSE	R^2	MSE	R^2	MSE	R^2
1	4.63	0.975	0.69	0.987	0.31	0.998
2	4.65	0.976	0.61	0.988	0.36	0.998
3	4.78	0.975	1.25	0.986	0.36	0.997
4	4.68	0.976	0.49	0.988	0.33	0.998
5	4.56	0.976	0.48	0.988	0.28	0.998
mean value	4.66	0.9756	0.82	0.9874	0.33	0.9978

Additionally, to visually illustrate the superior performance of the optimized prediction model, the dataset with the highest prediction accuracy from each model was selected for comparison.

The comparison results are shown in Figure 9.

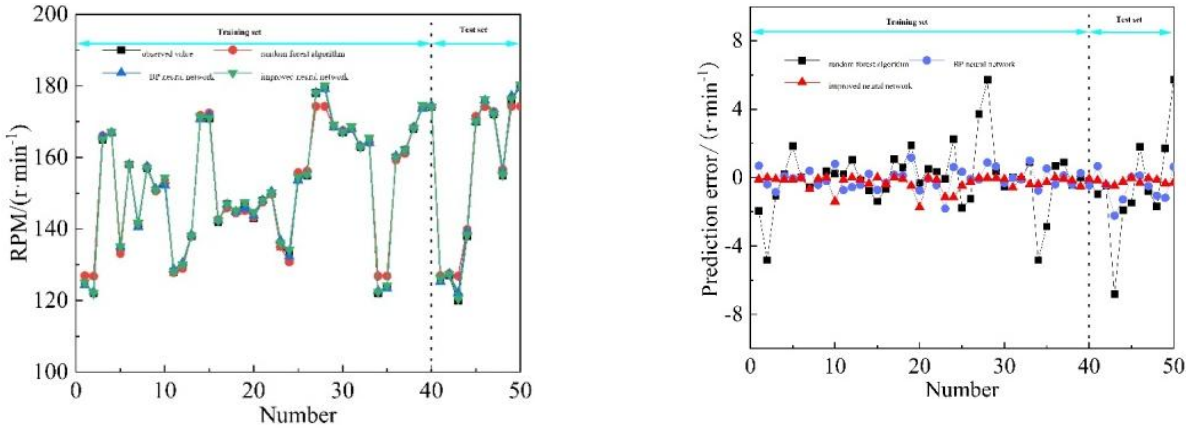

(a)Comparison of Optimal Rotational Speed Prediction.

(b) Comparison of Prediction Error

Figure 9. Comparative results of model predictions

Table 3 and Figure 9 indicate that the improved particle swarm optimization algorithm significantly enhances the predictive performance of the neural network model compared to both the random forest and the previous neural network models. The mean square error is reduced by 59.8% compared to the neural network model before optimization and 92.9% compared to the random forest model. The optimized neural network prediction model demonstrates enhanced stability and accuracy compared to its previous version. It enables better predictions of the optimal speed for the direct drive pump system of the submersible permanent magnet synchronous motor.

6 Conclusion

This article presents research on the optimal speed prediction algorithm for the system, selecting the neural network algorithm optimized by the improved particle swarm algorithm as the predictive model. The optimal rotational speed data for the system was obtained through experiments conducted on a simulated oil extraction platform. A comparative study was conducted on the random forest and neural network model predictions based on the experimental data. Optimization was performed to address the shortcomings of the neural network prediction algorithms. Introducing a dynamic inertia weight factor enhances global search capabilities, while the Cauchy mutation strategy improves local search efficiency and helps escape local optima. Simulation experiments demonstrate that the optimized neural network model significantly improves prediction accuracy, achieving a mean square error 59.8% lower than traditional models, with a determination coefficient of 0.998. These improvements enhance the practicality of predictive models and lay the groundwork for the research of control systems.

Reference

1. Brinner, T. R., McCoy, R. H., & Kopecky, T. (2013). Induction versus permanent-magnet motors for electric submersible pump field and laboratory comparisons. IEEE Transactions on Industry Applications,50(1), 174-181. https://doi.org/ 10.1109/TIA.2013.2288203
2. Mendoza-Mondragón, F., Hernández-Guzmán, V. M., & Rodríguez-Reséndiz, J. (2018). Robust speed control of permanent magnet synchronous motors using two-degrees-of-freedom control. IEEE Transactions on Industrial Electronics,65(8),6099-6108.https://doi.org/ 10.1109/TIE.2017.2786203
3. Yan, B., Wang, X., & Yang, Y. (2017). Starting performance improvement of line-start permanent-magnet synchronous motor using composite solid rotor. IEEE Transactions on Magnetics, 54(3), 1-4. https :// doi.org/10.1109/TMAG.2017.2753238
4. Huang, X., Tan, Q., Li, L., Li, J., & Qian, Z. (2016). Winding temperature field model considering void ratio and temperature rise of a permanent-magnet synchronous motor with high current density.IEEE Transactions on Industrial Electronics,64(3),2168-2177. https //doi.org/ 10.1109/TIE.2016.2625242
5. Pavlenko, V. (2008, October). Permanent magnet synchronous motor (PMSM)–New type of drives for submersible oil pumps. In SPE Russian Petroleum Technology

Conference?(pp. SPE-117375). SPE. https://doi.org/10.2118/117375-MS
6. Saveth, K., & Sagalovsky, A. (2013, August). Case histories of running progressing cavity pumps with submersible permanent magnet motors. In SPE Progressing Cavity Pumps Conference (pp. SPE-165654). SPE. https://doi.org/10.2118/165654-MS
7. Seczon, L., & Sagalovskiy, A. (2013, May). Field experience with the application and operation of permanent magnet motors in the ESP industry: success stories and lessons learned. In SPE Artificial Lift Conference-Latin America and Caribbean (pp. SPE-165 030). SPE.
8. Refai A, Abdou H A, Seleim A, et al. Permanent Magnet Motor application for ESP Artificial Lift [C]. North Africa Technical Conference and Exhibition 2013. Richardson: Society of Petroleum Engineers, 2013: 683-694. https://doi.org/10.2118/165030-MS
9. Grupping, A. W., Coppes, J. L. R., & Groot, J. G. (1988). Fundamentals of oilwell jet pumping.SPE Production Engineering,3(01), 9-14. https://doi.org/10.2118/15670-PA
10. Zhu, X., Song, J. G., & Zhang, Q. L. (2013). Investigation on all digital control system of brushless DC motor for beam-pumping unit.Applied Mechanics and Materials,336, 728-733. https://doi.org/10.4028/www.scientific.net/AMM.336-338.728
11. Siavashi, M., & Doranehgard, M. H. (2017). Particle swarm optimization of thermal enhanced oil recovery from oilfields with temperature control. Applied Thermal Engineering,123, 658-669. https://doi.org/10.1016/j.applthermaleng.2017.05.109.
12. Purkayastha, S. N., Gates, I. D., & Trifkovic, M. (2018). Real-time multivariable model predictive control for steam-assisted gravity drainage. AIChE Journal,64(8), 3034-3041. https://doi.org/10.1002/aic.16098
13. Min, W., Jiawei, W., Jinhui, G., Lihua, S., & Bogong, A. (2020). Multi-point prediction of aircraft motion trajectory based on GA-Elman-Regularization neural network. Integrated Ferroelectrics, 210(1), 116-127. https://doi.org/10.1080/10584587.2020.1728853
14. Liu, T., & Yin, S. (2017). An improved particle swarm optimization algorithm used for BP neural network and multimedia course-ware evaluation. Multimedia Tools and Applications 76, 11961-11974. https://doi.org/10.1007/s11042-016-3776-5
15. Hu, H., Zhai, X., Feng, J., & Guan, X. (2018, November). Prediction method of crude oil production based on FCM_GA_BP neural network. In 2018 IEEE 9th International Conference on Software Engineering and Service Science (ICSESS)(pp. 267-270). IEEE. https://doi.org/10.1109/ICSESS.2018.8663751
16. Li, X. , Chan, C. W. , & Nguyen, H. H. . (2013). Application of the neural decision tree approach for prediction of petroleum production. Journal of Petroleum Science & Engineering, 104(Complete), 11-16. 10. https://doi.org/10.1016/J.PETROL.2013.03.018
17. Lu, L., Liu, J., Huang, X., & Fan, Y. (2022). Gear fault diagnosis and life prediction of petroleum drilling equipment based on SOM neural network. Computational Intelligence and Neuroscience, 2022(1), 9841443. https://doi.org/10.1155/2022/9841443
18. Otchere, D. A., Ganat, T. O. A., Gholami, R., & Ridha, S. (2021). Application of supervised machine learning paradigms in the prediction of petroleum reservoir properties: Comparative analysis of ANN and SVM models. Journal of Petroleum Science and Engineering,200,108182. https://doi.org/10.1016/ j.petrol.2020.108182
19. Ye, Y., Yin, C. B., Gong, Y., & Zhou, J. J. (2017). Position control of nonlinear hydraulic system using an improved PSO based PID controller. Mechanical Systems and Signal Processing,83, 241-259. https://doi.org/10.1016/j.ymssp.2016.06.010